Spin−Orbit Coupling in Biradicals. 2.[1] Ab Initio Methodology and Application to 1,1-Biradicals: Carbene and Silylene

Zdeněk Havlas,[†] John W. Downing,[‡] and Josef Michl*,[‡]

Department of Chemistry and Biochemistry, University of Colorado, Boulder, Colorado 80309-0215, and Institute of Organic Chemistry and Biochemistry, Czech Academy of Sciences, Prague, Czech Republic

Received: December 8, 1997; In Final Form: March 24, 1998

A general procedure is described for the computation of spin−orbit coupling of triplet states of organic biradicals with their singlet states and of the zero-field splitting parameters of the triplets, including the full one- and two-electron terms of the Breit−Pauli Hamiltonian and using a new ab initio computer program suite. Spin−orbit coupling matrix elements are obtained for each triplet sublevel separately and are analyzed in an intuitively appealing fashion in terms of vectorial contributions from individual atoms and individual natural hybrid orbital pairs. CASSCF(6,6) results for S_0-T_1 spin−orbit coupling in CH_2 converge rapidly with increasing basis set size, and a polarized double-ζ basis set appears adequate. However, convergence with respect to the extent of electron correlation has not yet been reached at the CASSCF(6,6) level, whose results appear to be only semiquantitative. The experimental D' and E' values for CH_2 are reproduced within 5% at the CISD/aug-cc-pVTZ level, but the results obtained with less adequate electron correlation procedures and/or with smaller basis sets are only qualitatively correct. Results for spin−orbit coupling in CH_2 and SiH_2 as a function of the valence angle agree with expectations based on the algebraic 2-electrons-in-2-orbitals model of part 1. The T_1 parameters D' and E' in CH_2 and E' in SiH_2 are dominated by spin−spin dipolar coupling, whereas D' in SiH_2 is predicted to be dominated by spin−orbit coupling.

Introduction

Spin−orbit coupling is believed to be the main perturbation responsible for intersystem crossing (ISC) in short-chain triplet biradicals and therefore to be of key importance in numerous organic photochemical reactions. Although an early qualitative analysis[2] and numerous calculations[3] of spin−orbit coupling in organic biradicals have been published, it seemed to us that the qualitative structural understanding of spin−orbit coupling in these species was far from satisfactory. Particularly obscure were the exact nature of the role played by the delocalization of the singly occupied orbitals (A and B) into the saturated skeleton, its relation to the heavy atom effect, and the interference of terms provided by the individual atoms. For instance, our finding[4] that in the minimum basis set approximation the two-center through-space and one-center through-bond terms in twisted ethylene are of opposite signs suggested that qualitative understanding of structural effects on the rate of intersystem crossing in twisted olefins will be difficult to reach.

In a series of calculations, we found that spin−orbit coupling in a variety of organic biradicals can be conceptually reduced to spin−orbit coupling in 1,1- and 1,2-biradicals through the use of standard resonance structure arguments familiar to organic chemists, since the principal contributors are one-center terms mediated by through-bond coupling, together with a few of the two-center terms. Because of the critical role of through-bond coupling, increased understanding of spin−orbit coupling in biradicals will not only provide answers to problems in triplet photochemistry but also likely provide a useful and sensitive probe of σ electron structure in general. This structure is important in many contexts, such as energy and charge transfer, spin density and substituent effect propagation, linear and nonlinear optical properties, etc.

Because of the intricate interplay of spin−spin dipolar interaction with spin−orbit coupling in triplet states of organic molecules, we considered it desirable to include the calculation of zero-field splitting parameters. These quantities have been found useful for the characterization of organic biradicals, but their accurate computation is not easy.

The results are now reported in series of papers. The first article[1] presented a qualitative analysis of spin−orbit coupling in biradicals in terms of a 2-electrons-in-2-orbitals model amenable to algebraic solution and suggested an approach to the decomposition of computational results for spin−orbit coupling into intuitively understandable vectorial contributions from atoms and from hybrid orbital pairs. Next, for a group of prototype biradicals, we examine the structural and conformational dependence of spin−orbit coupling, test the validity of the simple model, and attempt to define the level of basis set and electron correlation treatment that are necessary to obtain reliable results.

For this purpose, we assembled a new computer program that permits us to analyze the results in qualitative terms. In addition to being able to handle larger basis sets and more extensive configuration interaction than was possible in much of the earlier work on larger biradicals,[3] the program differs from those already available in two main points:

(i) The three sublevels of T_1 (T_x, T_y, and T_z) for which the spin−orbit coupling matrix elements are calculated are chosen as the eigenstates of the spin−spin dipolar coupling operator, permitting a comparison of separate ISC rates for each real triplet sublevel. This takes advantage of the usual dominance of the spin−spin dipolar interaction in determining the zero-field splitting in triplet states of organic molecules. The

[†] Czech Academy of Sciences.
[‡] University of Colorado.

S1089-5639(98)00460-5 CCC: $15.00
Published on Web 05/29/1998

procedure is essential in the general case, particularly if the initial triplet generation occurs by intersystem crossing from the singlet manifold. It is unnecessary only if relaxation among the three levels is fast relative to the triplet lifetime, and only the overall intersystem crossing rate is of interest. Since T_x, T_y, and T_z diagonalize the spin−spin dipolar Hamiltonian in the absence of an external magnetic field, they provide natural molecular axes *x*, *y*, and *z*. In small-molecule calculations, the simultaneous consideration of the spin−spin dipolar and spin−orbit coupling operators has become standard,[5] but in spin−orbit calculations on larger molecules of low symmetry, molecular axes have usually been chosen arbitrarily and only the root-mean-square value, SOC, was computed. When all three values were reported,[6] they had no individual physical significance.

(ii) To facilitate a direct comparison with results of the algebraic model, the calculations are performed in an MO basis that incorporates the most localized form of the two "open-shell" orbitals, and both the one-electron and the two-electron contributions of $\hat{H}^{SO}$ to $\langle T_x|\hat{H}^{SO}|S_0\rangle$, $\langle T_y|\hat{H}^{SO}|S_0\rangle$, and $\langle T_z|\hat{H}^{SO}|S_0\rangle$ are analyzed in terms of increments provided by individual atoms and by pairs of natural hybrid orbitals (NHOs)[7] on those atoms.[8] The NHO analysis is more general than an earlier attempt[9] to separate through-space and through-bond contributions to spin−orbit coupling by comparison of the results for the actual biradical with those for a methyl radical pair, since in some conformations the methyl groups interpenetrate severely and the two radical centers are not really independent. Also, the finding[9] that the through-space and through-bond contributions are roughly proportional to each other in the trimethylene biradical, which led its authors to propose a simple semiempirical formula for spin−orbit coupling in biradicals, need not be valid generally. We found Weinhold's natural bond orbitals very useful previously for understanding long-range spin density propagation in [*n*]staff-3-yl radicals.[10] In the present context, the analysis permits a clear distinction of through-space and through-bond contributions to the overall spin−orbit coupling mechanism.

In the present paper, the testing is performed on a 1,1-biradical, CH_2, and the results are compared with those for SiH_2. There has not been much previous computational work on spin−orbit coupling in these molecules.[11] McKellar et al.[12] calculated spin−orbit coupling matrix elements between the lowest triplet ($^3B_1$) and lowest singlet ($^1A_1$) electronic states of CH_2 using the full Breit−Pauli operator for three different valence angles. The best values were obtained with the [7s4p2d/3s2p] basis set and CISD wave function with perturbation-based selection of doubly excited configurations (90°, 13.068 cm^{-1}; 112°, 13.182 cm^{-1}; 135.1°, 11.840 cm^{-1}). These values were used to calculate rovibronic matrix elements of the spin−orbit coupling operator for the interpretation of spectra of CH_2.[12,13] These SOC values, increased by a factor of 5.08 obtained from the ratio $\zeta_{SO}(SiH)/\zeta_{SO}(CH)$, were also used to analyze the experimental data obtained for SiH_2.[14]

Prior computational results for the zero-field splitting parameters in triplet CH_2 were first obtained at the "spin−spin-only" level[15−17] (*D*, *E*) for a range of valence angles. Subsequent results were obtained[18] for two valence angles with inclusion of corrections for spin−orbit coupling (*D*′, *E*′), using an unpolarized double-ζ quality basis set and CI with singly and selected doubly excited configurations. The correction that converts *D* to *D*′ was found to be relatively unimportant, and the correction that converts *E* to *E*′ was entirely negligible. A gradual increase of the *D* value with an increasing valence angle was attributed to increasing spin−spin dipolar interaction. Good agreement with experiment was found: the computed values were $|D'| = 0.807$ cm^{-1} and $|E'| = 0.049$ cm^{-1}, while the experimental values deduced[19] from an analysis of a large number of studies are $|D'| = 0.79 \pm 0.02$ $cm^{-1}$and $|E'| = 0.05 \pm 0.02$ cm^{-1}. Recently, more accurate values were obtained from laser magnetic resonance measurements on CHD:[20] $|D'| = 0.7567$ cm^{-1}, and $|E'| = 0.0461$ cm^{-1}, and for these, the agreement is a little less impressive.

No calculations of zero-field splitting parameters seem to have been performed for triplet SiH_2, and no direct observations are available.

Calculational Procedures

Previously Available Programs. Most of the readily available ab initio codes for general polyatomic molecules (GAMESS,[21] MELD,[22] GAUSSIAN,[23] CADPAC,[24] etc.) are able to calculate one-electron spin−orbit matrix elements, as are some semiempirical programs.[25−27] In contrast, only a few ab initio programs have the two-electron part of the spin−orbit coupling operator incorporated, and we next list those that we are aware of. As far as we know, Langhoff[18] and King with Furlani (SOCC program)[28] wrote the first CI codes for calculations on polyatomic biradicals that included both parts of the spin−orbit coupling Hamiltonian. Yarkony et al.[5] developed a large-scale CI code for both spin−orbit and spin−spin dipolar coupling, Handy, Palmieri, and collaborators[29] added spin−orbit coupling code to the SCF level of the CADPAC[24] program, Ågren et al.[30,31] programmed spin−orbit coupling for response function theory, and Peyerimhoff et al.[32] incorporated spin−orbit coupling code into the MRD-CI program.

The New Program. A new ab initio program suite (SOSS) has been written for the calculation of spin−orbit and spin−spin coupling matrix elements by modifying the GAMESS[21] program of Gordon. The spin−orbit part was added from the SOCC[28] program of Furlani and King, the spin−spin part originated in the MELD[22] program of Davidson and Feller, and the natural bond orbital part was adapted from the NBO[33] program of Weinhold. The version of the SOCC program that we obtained was first modified by Jacobs and Caldwell.[34] We modified it further and included a decomposition into contributions from pairs of Weinhold's[33] natural hybrid orbitals.[4,35,36] The Furlani−King SOCC program has also been modified by Zimmerman, Kutateladze, and collaborators,[6,8,37] who independently of us developed the concept of analysis of spin−orbit coupling results in terms of pairs of natural hybrid orbitals.

The sequence of steps in our calculations is as follows: (i) MCSCF (usually CASSCF) or ROHF-CI wave functions are obtained for the singlet and triplet states of interest in terms of the most localized orbitals for the open shell of the triplet state; (ii) the spin−spin dipolar coupling tensor is computed and diagonalized for the triplet, providing a definition of the T_x, T_y, and T_z triplet wave functions, the set of principal magnetic molecular axes, and the spin−spin-only values *D* and *E*; (iii) the spin−orbit coupling matrix elements for each of the three triplet components with the singlet state are computed, including both one- and two-electron terms, and can be used to estimate the rates of intersystem crossing from each of the triplet components to the singlet, using Fermi's golden rule; (iv) the spin−orbit results are expressed as a sum over pairs of natural hybrid orbitals and a sum over atomic contributions for purposes of qualitative analysis and understanding; and (v) the mixing of the S and T levels by the matrix elements of the spin−orbit operator between singlets and the lowest triplet is evaluated to

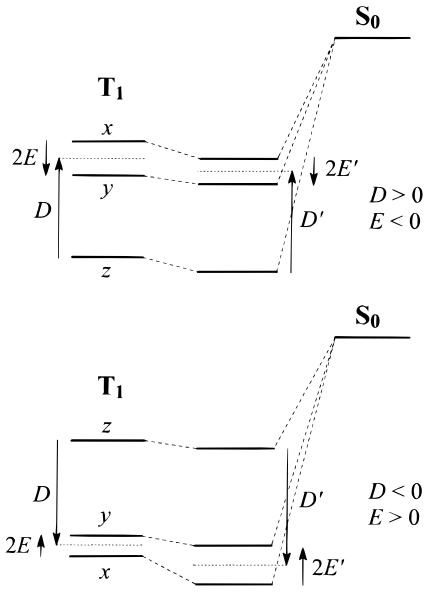

Figure 1. Relation of "spin−spin-only" (D, E) and "spin−spin plus spin−orbit" (D', E') values of zero-field splitting parameters to energies of triplet sublevels. S_0-T_1 mixing only, S_0 assumed above T_1 in energy. The EPR axis labeling convention[19] is used.

obtain the final state energies, the final (observable) zero-field splitting parameters D' and E' for the triplet, and the final directions of molecular magnetic axes.

The five steps are next described in more detail:

(i) The GAMESS program is used to generate wave functions of the singlet and triplet to be used for the evaluation of the spin−spin and spin−orbit matrix elements. When the present calculations were performed, the memory available on our computers limited the CASSCF procedure to 6 electrons in 6 orbitals at most; now, 8 electrons in 8 orbitals can be treated. The BKKM[38] orbital localization is used to rotate the two singly occupied orbitals of the triplet open shell to produce the most localized pair. This guarantees maximum compatibility with the algebraic model of part 1.[1] The MOs generated, either ROHF or MCSCF, are converted into the MELD format. In general, these MOs are different for the singlet and the triplet state.

(ii) The spin−spin dipolar coupling tensor elements are computed using the appropriate term in the Breit−Pauli Hamiltonian (without the Fermi contact interaction term):[39]

$$\hat{H}^{SS} = \frac{e^2\hbar^2}{m^2c^2}\sum_{i<j}\frac{r_{ij}^{\,2}(\boldsymbol{s}_i\cdot\boldsymbol{s}_j) - 3(\boldsymbol{r}_{ij}\cdot\boldsymbol{s}_i)(\boldsymbol{r}_{ij}\cdot\boldsymbol{s}_j)}{r_{ij}^{\,5}} \tag{1}$$

where $\boldsymbol{r}_{ij} = \boldsymbol{r}_i - \boldsymbol{r}_j$.

The MELD program evaluates the five independent elements of the symmetric, traceless, 3×3 spin−spin dipolar interaction matrix in five independent runs.[40] Diagonalization of the resulting matrix provides the "spin−spin-only" approximation to the orientation of the principal magnetic molecular axes, as well as to the D and E zero-field splitting parameters: $D = -(3/2)Z$ and $E = -(1/2)(X - Y)$, where X, Y, and Z are the eigenvalues associated with the magnetic axes x, y, and z, respectively. In the convention used[19] (Figure 1), the labels of the axes are chosen so as to make $|D| \geq |3E|$ and $DE < 0$. Then, T_z is the lowest and T_x the highest in energy if $D > 0$, and the level order is the opposite if $D < 0$. These principal axes are used in all subsequent steps dealing with the zero-field splitting parameters of the triplet. In some plots, variation in molecular geometry would cause the correct label to switch within the plot as the relative size of the zero-field splitting parameters changes, causing considerable confusion, and we then prefer to keep throughout the labels that are appropriate for most of the plot.

At times, the labels of the axes that are imposed by the EPR convention for the magnitudes and signs of D and E[19] differ from those usually adopted in other types of spectroscopy (e.g., when only one 2-fold symmetry axis is present, it is normally called z). Their general adoption would force a change of state group symmetry symbols relative to the usual ones and would lead to likely confusion. We see no easy way to satisfy the clashing conventions and adopt a procedure that calls for the use of the usual axis labeling system except when explicitly discussing EPR D and E terms.

(iii) The SOCC program uses the corresponding orbital procedure[28] to calculate the $\langle {}^3\Psi|\hat{H}^{SO}|{}^1\Psi\rangle$ matrix elements using the spin−orbit term in the Breit−Pauli Hamiltonian:[39]

$$\hat{H}^{SO} = \frac{e^2\hbar}{2m^2c^2}\left[\sum_{i,\alpha}\frac{Z_\alpha}{r_{i\alpha}^{\,3}}(\boldsymbol{r}_{i\alpha}\times\boldsymbol{p}_i)\cdot\boldsymbol{s}_i - \sum_{i,j\neq i}\frac{(\boldsymbol{r}_{ij}\times\boldsymbol{p}_i)}{r_{ij}^{\,3}}\cdot(\boldsymbol{s}_i + 2\boldsymbol{s}_j)\right] \tag{2}$$

where $\boldsymbol{r}_{i\alpha} = \boldsymbol{r}_i - \boldsymbol{r}_\alpha$.

The formula tape generator of the SOCC program (FORMFAC program) is not equivalent to the GUGA formalism used in the GAMESS program, and therefore the CI wave function has to be converted. The GAMESS CI wave function can be transformed into the FORMFAC form

$$|\Omega_I^{\,G}\rangle = \sum_K |\Omega_K^{\,F}\rangle\langle\Omega_K^{\,F}|\Omega_I^{\,G}\rangle \tag{3}$$

where Ω_I^G (Ω_K^F) is the GAMESS (FORMFAC) configuration state function (CSF). The final formula for FORMFAC expansion coefficient Q_I^F of the CI wave function in terms of CSFs ($\Psi^F = \sum_I Q_I^F\ \Omega_I^F$) requires only the knowledge of the determinants (Δ_m, Δ_n) forming the CSFs (I, K) and their expansion coefficients in the CSFs ($C_n^{G,I}$, $C_m^{F,K}$):

$$Q_K^F = \sum_I^{G'} Q_I^G \sum_n^{N^G} C_n^{G,I} \sum_m^{N^F} Q_m^{F,K}\langle\Delta_n^{G,I}|\Delta_m^{F,K}\rangle \tag{4}$$

The first summation runs over CSFs with equal occupation numbers of the molecular orbitals. The integral $\langle\Delta_n^{G,I}|\Delta_m^{F,K}\rangle$ is equal to unity if both determinants are identical and otherwise vanishes.

Most ab initio programs, including GAMESS, generate high-spin wave functions for multiplicity higher than zero; in the case of triplet CI wave functions, this is $M_s = 1$. For the evaluation of the x and y components of the spin−orbit coupling matrix elements the triplet wave function for $M_s = 0$ is required. This is constructed by application of the spin-down operator $\hat{S}_- = \hat{S}_x - i\hat{S}_y$ [$\hat{S} = \sum_i \hat{s}(i)$], followed by the projection of the resulting wave function into the space of the FORMFAC CSFs.

(iv) Weinhold's NBO[33] program has been added to GAMESS. To analyze the origin of the spin−orbit coupling constant, the one- and two-electron contributions are transformed into Weinhold's (atom, hybrid, or bond, orthogonal or preorthogonal) natural orbitals.[7]

The one-electron spin−orbit matrix elements H_1^{SO} are transformed to one of the Weinhold bases according to

$$H_1^{SO} = \sum_{\rho,\sigma} h_{\rho\sigma}^{(1)W} = \sum_{\rho,\sigma} T_{\rho\sigma}^{W} I_{\rho\sigma}^{W} \tag{5}$$

where the quantities with a superscript W are calculated in the basis of Weinhold orbitals, $T_{\rho\sigma}^{W}$ is an element of the one-particle transition density matrix,[28,41] and $I_{\rho\sigma}^{W}$ are the one-electron spin−orbit integrals. The dependence of these quantities on M_s (or x, y, z) is made implicit for simplicity. If we express the MOs in terms of AOs as $\varphi_i = \sum_\mu c_{i\mu}\chi_\mu$ and Weinhold orbitals in terms of AOs as $\tau_\rho = \sum_\mu u_{\rho\mu}\chi_\mu$, the values of $T_{\rho\sigma}^{W}$ and $I_{\rho\sigma}^{W}$ can be readily obtained from the AO transition density matrix and integrals by the following transformations:

$$\mathbf{T}^{W} = (\mathbf{u}^{-1})^{\dagger}\cdot\mathbf{T}^{AO}\cdot(\mathbf{u}^{-1}), \quad \mathbf{I}^{W} = \mathbf{u}^{\dagger}\cdot\mathbf{I}^{AO}\cdot\mathbf{u} \tag{6}$$

The sum $\tilde{h}_{\rho\sigma}^{(1)} = h_{\rho\sigma}^{(1)} + h_{\sigma\rho}^{(1)}$ is then the contribution from the Weinhold orbital pair ρ,σ ($\rho \geq \sigma$) to the one-electron part of spin−orbit coupling. Because the one-electron spin−orbit Hamiltonian is a sum of contributions from nuclei, $H_1^{SO} = \sum_\alpha H_1^{SO}(\alpha)$, we further collect the orbital contributions into atomic contributions $\tilde{h}_{\rho\sigma}^{(1)}(\alpha)$: $\tilde{h}_{\rho\sigma}^{(1)} = \sum_\alpha \tilde{h}_{\rho\sigma}^{(1)}(\alpha)$.

The two-electron contributions are transformed into the Weinhold basis in a similar way,

$$H_2^{SO} = \sum_{\mu,\nu,\rho,\sigma} h_{\mu\nu\rho\sigma}^{(2)W} = \sum_{\mu,\nu,\rho,\sigma} T_{\mu\nu\rho\sigma}^{W} I_{\mu\nu\rho\sigma}^{W} \tag{7}$$

The two-particle transition density matrix is calculated using the expansion coefficients of the molecular orbitals in terms of the Weinhold orbitals, $\mathbf{t} = \mathbf{C}^{\dagger}\cdot(\mathbf{u}^{-1})$. The two-electron, four-center integral transformation is a task similar to the MO transformation in CI programs,[42] and a similar procedure was applied. The only difference is the symmetry of the two-electron spin−orbit integrals, which are antisymmetric with respect to exchange of orbitals occupied by electron 1 and symmetric with respect to the exchange of orbitals occupied by electron 2. The program performs the integral transformation and transition density matrix reevaluation for each of the desired Weinhold orbital sets and prints two quantities: first, the four index contribution $\tilde{h}_{\mu\nu\rho\sigma}$, which is the sum of all elements with indices μ, ν, ρ, σ in any order and is useful for analysis of the total screening effect of the core orbitals; second, the orbital pair contribution $h_{\rho\sigma}^{(2)}$:

$$\tilde{h}_{\rho\sigma}^{(2)} = {}^1/_6 \sum_{\mu\geq\nu} (\tilde{h}_{\rho\sigma\mu\nu} + \tilde{h}_{\rho\mu\sigma\nu} + \tilde{h}_{\rho\mu\nu\sigma} + \tilde{h}_{\mu\rho\sigma\nu} + \tilde{h}_{\mu\rho\nu\sigma} + \tilde{h}_{\mu\nu\rho\sigma}) \quad (\rho \geq \sigma) \tag{8}$$

where the elements $\tilde{h}_{\mu\nu\rho\sigma}$ are nonzero only if $\mu \geq \nu \geq \rho \geq \sigma$. The weight factor $^1/_6$ corrects for the fact that each element $\tilde{h}_{\mu\nu\rho\sigma}$ contributes to six different orbital pairs. Finally, the value $\tilde{h}_{\rho\sigma} = \tilde{h}_{\rho\sigma}^{(1)} + \tilde{h}_{\sigma\rho}^{(2)}$ ($\rho \geq \sigma$) is computed. In the determination of total atomic contributions $\tilde{h}(\alpha)$, we divide $\tilde{h}_{\sigma\rho}^{(2)}$ equally between atoms that carry orbitals σ and ρ: $h(\alpha) = \tilde{h}^{(1)}(\alpha) + \sum_{\sigma(\alpha)} \tilde{h}_{\sigma\rho}^{(2)}/2$, where the sum runs only over those orbitals σ that are carried by atom α.

The simplification of the two-electron part to only two orbital subscripts is possible because in all nonnegligible contributions two of the four orbitals are always twice an inner core orbital on a single atom. These contributions thus describe the interaction of hybrid pairs screened by inner electrons. The core orbitals are quite independent of the chemical environment, and the screening effect is dictated by the nature of the atom on which the hybrid pair is located.

(v) The mixing of the triplet and singlet levels of a biradical by the spin-dependent terms in the Hamiltonian is treated approximately. Only the elements of the spin−orbit coupling operator between the three levels of the lowest triplet and at least the lowest three singlets are considered, while its elements between the lowest and higher triplets and elements between triplets and quintets are ignored. This approximation is obviously exact for the 2-in-2 description of biradicals, used in the model of part 1.[1] We also ignore all elements of the spin−spin dipolar coupling operator that connect different states. It is hoped that these neglects are acceptable when the properties of the lowest triplet are to be described, even though we realize that in at least one case (predissociation of NH)[43] first-order spin−spin dipole induced singlet−quintet state mixing is known to dominate over second-order spin−orbit induced mixing of the same states.

The approximate Hamiltonian matrix is diagonalized to yield the spin−orbit corrected energies of the three sublevels of the lowest triplet, X', Y', and Z', from which the corrected zero-field splitting parameters D' and E' are calculated in the usual manner (Figure 1) for comparison with experiment. In the rare event that the difference $2J$ of the average energy of the three triplet sublevels and the singlet energy would be comparable to the spin−orbit coupling matrix elements (J is the "exchange integral"), a four-level instead of the usual three-level problem would result, and the D' and E' parameters could then not be determined from experiment. It would be necessary to fit the measured EPR spectra not only with the parameters D and E but also with J and the spin−orbit coupling matrix elements. This situation is characterized by a divergence of the D' and E' values computed from the usual formulas (Figure 1) at points of first-order singlet−triplet degeneracy.

The present program computes spin−spin and spin−orbit interaction as a function of nuclear geometry but does not average them over vibrational wave functions.

Application to Carbene and Silylene. All computations were performed at geometries optimized for the state of primary interest, the lowest triplet. The bond lengths of CH_2 and SiH_2 were optimized for a series of valence angles α from 60° to 180°, using B3LYP/cc-pVTZ and assuming C_{2v} (or $D_{\infty h}$) symmetry. The minima occurred at $d_{CH} = 1.0774$ Å, $\alpha_{HCH} = 135.0°$ and $d_{SiH} = 1.4872$ Å, $\alpha_{HSiH} = 118.6°$. These results compare well with the experimental values[44] for triplet CH_2 ($d_{CH} = 1.0766$ Å, $\alpha_{HCH} = 134.0°$) and the results of large basis set CEPA calculations[45] for triplet SiH_2 ($d_{SiH} = 1.4793$ Å, $\alpha_{HSiH} = 118.4°$), respectively. The location of the magnetic axes is dictated by symmetry, and the calculations showed that the convention[19] described above requires that x be the out-of-plane axis, that y be the 2-fold symmetry axis, and that z lie parallel to the H−H line. This differs from the usual axis labeling in these molecules in that the y and z axes are interchanged.

Calculations of spin−spin dipolar coupling and spin−orbit coupling for CH_2 were performed at the CASSCF(6,6) level for a variety of basis sets, starting with the minimum STO-3G basis up to the correlation-consistent triple-ζ basis set (cc-pVTZ). The spin−spin dipole interaction elements were also calculated for several basis sets with ROHF, CIS, CASSCF(6,6), CISD, and CISDTQ wave functions. The size of the CI expansion ranged from 1 (ROHF) to 461 916. Less extensive calculations were performed for SiH_2. Natural orbital analysis was based on triplet MOs.

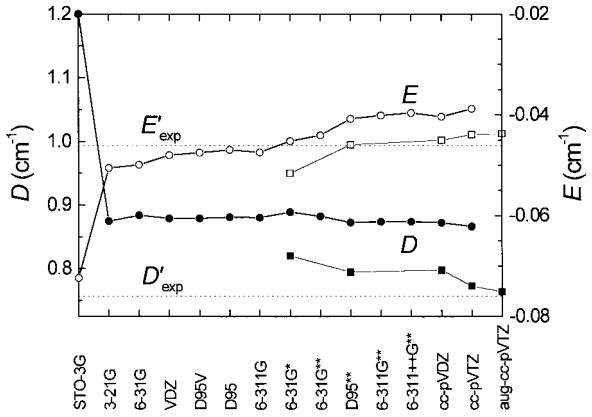

Figure 2. Triplet carbene "spin−spin-only" zero-field splitting parameters *D* (solid symbols) and *E* (open symbols) calculated at the CASSCF(6,6) (circles) and CISD (squares) levels at triplet-optimized geometry. Best experimental values are represented by dotted lines. The EPR axis labeling convention[19] is used.

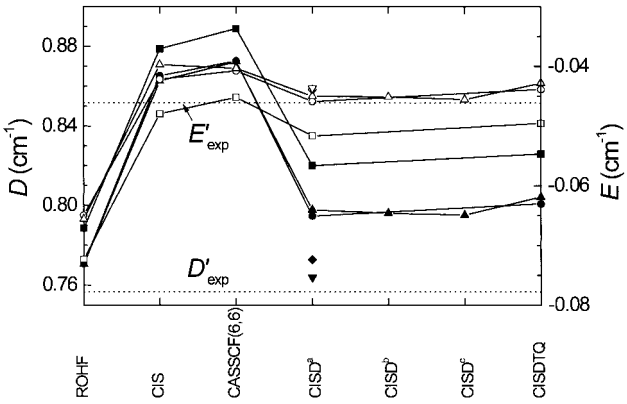

Figure 3. Triplet carbene "spin−spin-only" zero-field splitting parameters *D* (solid symbols) and *E* (open symbols) calculated using different wave functions and basis sets (■, 6-31G**; ●, D95**; ▲, cc-pVDZ; ♦, cc-pVTZ; ▼, aug-cc-pVTZ) at triplet-optimized geometry. CISD wave function was derived from all orbitals (c), all orbitals except frozen core orbital on carbon (b), or all orbitals except frozen core and virtual orbitals on carbon (a). Best experimental values are represented by dotted lines. The EPR axis labeling convention[19] is used.

The calculations used IBM RS6000/590 and SGI Power Challenge and Octane computers.

Results

Effects of Basis Set Size and of Electron Correlation Treatment. Our first task was to determine which level of calculation is necessary for our purposes, i.e., for qualitative interpretation of the course of photochemical reactions, and, if possible, which level is necessary for achieving quantitative agreement with experiments. The testing was performed on CH_2 and was based, first, on the convergence of the computed values as the quality of the computational procedure was improved and second, on agreement with the observed[20] zero-field splitting parameters D' and E'. As we shall see below, these are determined nearly exclusively by the "spin-spin-only" D and E values ($D' \approx D + 0.023$ cm^{-1}, $E' \approx E + 0.0001$ cm^{-1}) and can be used to test the quality of the calculation of the spin−spin dipolar tensor. D and E values of carbene obtained for a series of basis sets using CASSCF(6,6) and CISD wave functions and the EPR axis labeling convention[19] are shown in Figure 2. Except for the hopelessly inaccurate STO-3G basis set, they all produce values in the right range for both D and E. The former is positive and the latter negative, and the top part of Figure 1 applies.

Although D values between 0.8 and 0.9 cm^{-1} are qualitatively acceptable compared to the observed[20] value of $|D'| = 0.7567$ cm^{-1}, only CISD with the larger among the basis sets yields values below 0.8 cm^{-1}. Even the largest of the triple-ζ basis sets cannot be claimed to provide a fully converged result, and larger basis sets would probably produce somewhat smaller D values. The CISD/aug-cc-pVTZ result for D agrees with the observed D' value within 1%, but when we remember the need to correct the latter for the effects of spin−orbit coupling, we see that the computed D value is still too high by approximately 0.036 cm^{-1}, i.e., about 5%. It thus appears that at the CISD level the correct answer will most likely result with a quadruple- or pentuple ζ basis set. Judging by the results shown in Figure 3, which illustrate the dependence of the calculated D and E values (with the EPR axis labeling convention[19]) on the extent of electron correlation, from one-determinantal (ROHF) and CIS to CASSCF(6,6) and CISDTQ wave functions, CISD represents the minimum acceptable level of electron correlation treatment if quantitative agreement with experiment is desired. Fortunately, it appears that freezing the core or virtual orbitals hardly affects the results. The slight increase in the computed value of D upon going from CISD to CISDTQ suggests that even larger basis sets may well be needed to obtain exact agreement with experiment at the latter level compared with the former, if the trend apparent in Figure 2 continues.

Since the spin−orbit correction to E is computed to be entirely negligible, the calculated values can be compared directly to the observed value of $|E'| = 0.0461$ cm^{-1}, and it is seen in Figure 2 that nearly all methods of calculation produce a qualitatively satisfactory result between −0.04 and −0.05 cm^{-1}. Quantitative agreement is however again not reached. Improvements in the basis set bring the calculated E value closer to zero, and convergence is most likely not yet reached at the triple-ζ level. This trend is initially compensated by an improvement in electron correlation treatment. Even at the CISD level, however, the E value is too close to zero, and Figure 3 suggests that going to CISDTQ will bring it even closer. It is not clear how the exact experimental value will be reached as the calculation is improved further, and it is conceivable that vibrational averaging will be necessary. It is some consolation to note that the 5% error in our best CISD/aug-cc-pVTZ calculation for E represents only 0.002 cm^{-1} and actually is 15 times smaller than the error in our best calculation for D.

Figure 4, which uses the usual axis labels, shows the results of CASSCF(6,6) calculations of spin−orbit coupling matrix elements involving the lowest B_1 triplet state and the first six singlet states ($1A_1$, B_1, $2A_1$, A_2, B_2, $3A_1$). The double-ζ basis seems to be the minimum requirement, but for quantitative results triple-ζ or better basis sets are necessary. The inclusion of polarization functions on the carbon atom in the basis set has a noticeable effect on spin−orbit matrix elements. Not surprisingly, the hydrogen polarization functions have virtually no effect because the singly occupied orbitals of carbene, which are responsible for the main contribution to the spin−orbit matrix elements, are strongly localized on the carbon atom. In general, a fully polarized basis set might be necessary. The inclusion of diffuse functions changes the matrix elements only slightly.

The situation is less favorable with regard to the treatment of electron correlation. Figure 5 shows that the values of the spin−orbit coupling matrix elements are probably not yet converged at the CASSCF(6,6) level and that a better treatment will most likely be necessary for quantitative agreement. One

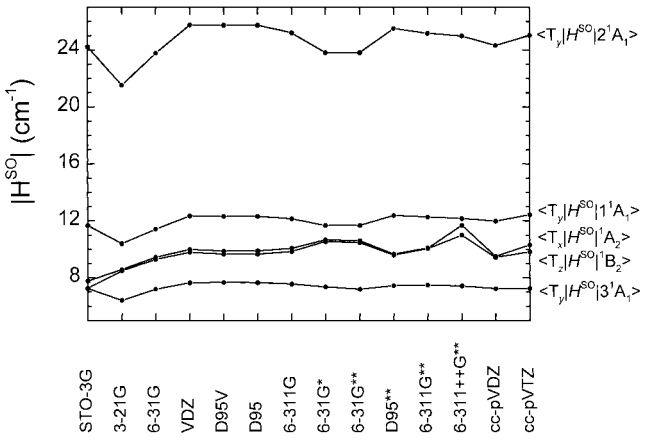

Figure 4. Triplet carbene. Basis set dependence of T_1-S_n spin−orbit matrix elements at triplet-optimized geometry, CASSCF(6,6). The usual axis labeling convention is used.

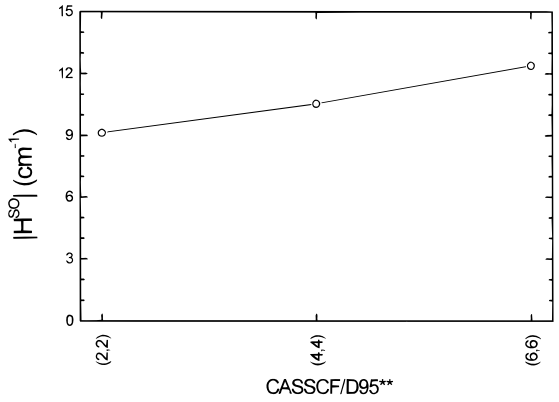

Figure 5. Triplet carbene. Effect of the extent of electron correlation on T_1-S_0 spin−orbit matrix element at triplet-optimized geometry, D95** basis set.

can hope, however, that qualitative trends will be reproduced even with this procedure.

Effect of One versus Two Orbital Sets. Our program calculates spin−orbit coupling matrix elements using either one or two molecular orbital sets. In the former case the triplet CASSCF orbitals are used to generate both the triplet and the singlet CI wave functions. In the latter case triplet and singlet CASCSF optimized orbitals are used for the triplet and singlet CI wave functions, respectively, except that a common set of core orbitals is used (usually the triplet orbitals). Triplet−singlet matrix elements are calculated by the method of corresponding orbitals,[46,47] formulated in such a way that the maximally localized[38] nature of the triplet orbitals is preserved. In the present article we report results obtained with two CASSCF orbital sets, optimized for the lowest triplet and singlet states. One orbital set calculations for CH_2 give qualitatively similar results for the matrix elements involving the lowest singlet states. Only the 3^1A_1 singlet state, which strongly interacts with higher lying $^1A_1$ states, gives very different results. For bending angles between 60° and 180° the average (maximum) difference between these two kinds of calculations for $1A_1$, $2A_1$, A_2, and B_2 singlet states is 0.7 cm^{-1} (1.9 cm^{-1}). The difference is largest for the smallest and largest bending angles.

Effects of Bending. Results of CASSCF(6,6)/D95** calculations of the energies of the lowest triplet and six lowest singlets of CH_2 and SiH_2 as a function of the valence angle α, at geometries optimized for the lowest triplet, are shown in Figures 6 and 7, respectively (with state labels based on the usual axis labels). Matrix elements of the spin−spin (Figures 8 and 9, the EPR convention for axis labels) and spin−orbit (Figures 10 and 11, the usual convention for axis labels) operators were calculated at these geometries at the same level of theory. The spin−spin matrix elements were also calculated in the CISD/D95** approximation (Figures 8 and 9). The signs of the matrix elements of H^{SO} are arbitrary in that they are

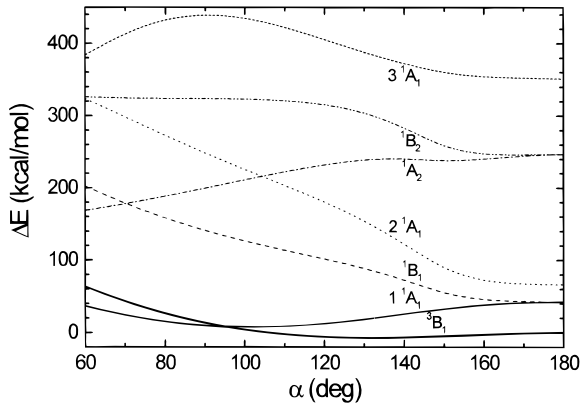

Figure 6. Carbene. CASSCF(6,6)/D95** energies of the lowest triplet state and six lowest singlet states at triplet-optimized geometries as a function of the valence angle α. The usual axis labeling convention is used.

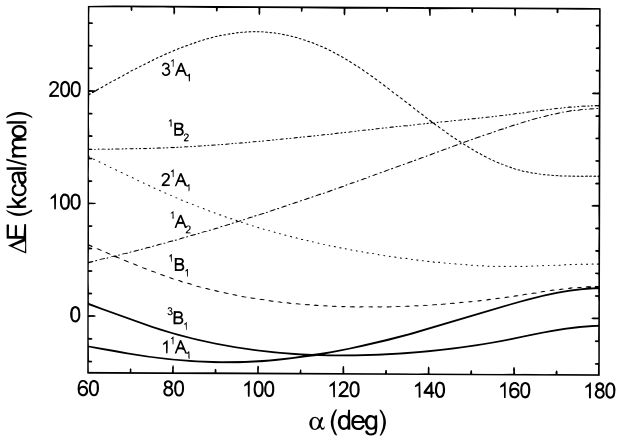

Figure 7. Silylene. CASSCF(6,6)/D95** energies of the lowest triplet state and 6 lowest singlet states at triplet-optimized geometries as a function of the valence angle α. The usual axis labeling convention is used.

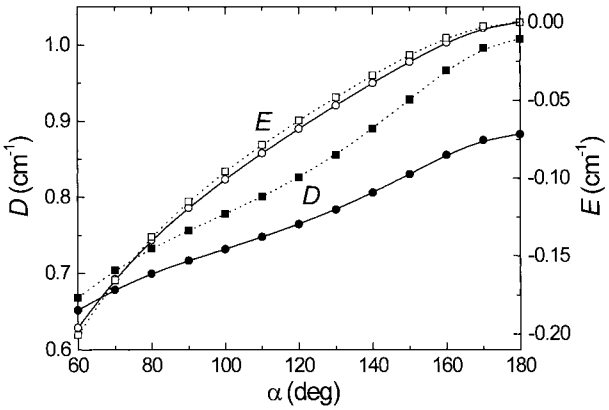

Figure 8. Triplet carbene "spin−spin-only" zero-field splitting parameters *D* (solid symbols) and *E* (open symbols) calculated at triplet-optimized geometries as a function of the valence angle α at the CISD/D95** (solid line) and CASSCF(6,6)/D95** (dashed line) levels. The EPR axis labeling convention[19] is used.

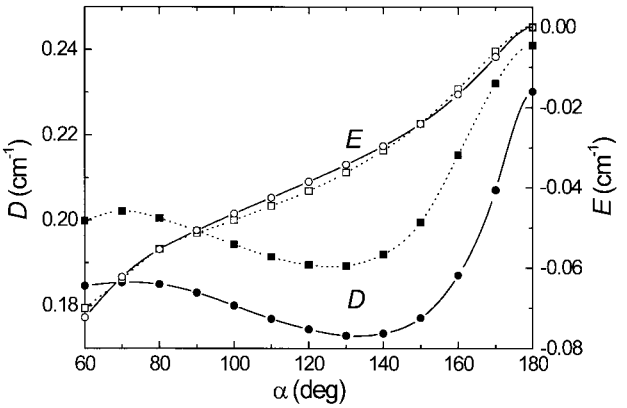

Figure 9. Triplet silylene "spin−spin-only" zero-field splitting parameters *D* (solid symbols) and *E* (open symbols) calculated at triplet-optimized geometries as a function of the valence angle α at the CISD/D95** (solid line) and CASSCF(6,6)/D95** (dashed line) levels. The EPR axis labeling convention[19] is used.

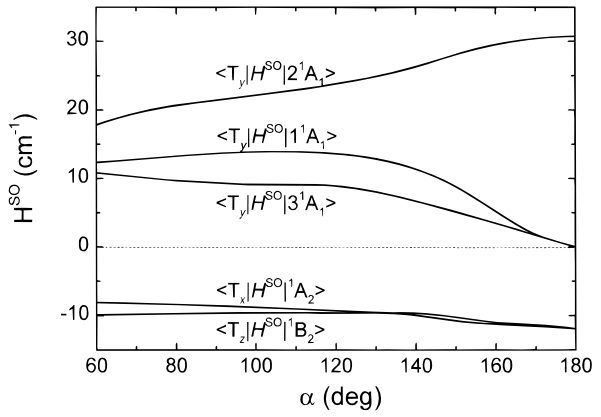

Figure 10. Carbene spin−orbit matrix elements $\langle T_1|\hat{H}^{SO}|S_n\rangle$ calculated at triplet-optimized geometries at the CASSCF(6,6)/D95** level as a function of the valence angle α. The usual axis labeling convention is used.

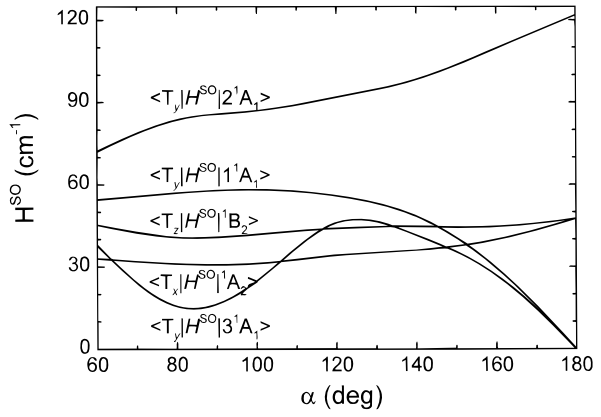

Figure 11. Silylene spin−orbit matrix elements $\langle T_1|\hat{H}^{SO}|S_n\rangle$ calculated at triplet-optimized geometries at the CAS-SCF(6,6)/D95** level as a function of the valence angle α. The usual axis labeling convention is used.

dictated by the choice of wave function phase. We have chosen them so as to minimize crowding in the drawing.

Effects of Spin−Orbit Coupling on Zero-Field Splitting Parameters. The interplay of terms in the determination of the zero-field splitting parameters for the lowest triplet T_1 was examined using the D95** basis set, CISD wave functions in the calculation of the diagonal spin−spin matrix elements *X*, *Y*, and *Z*, and CASSCF(6,6) wave functions in the calculation

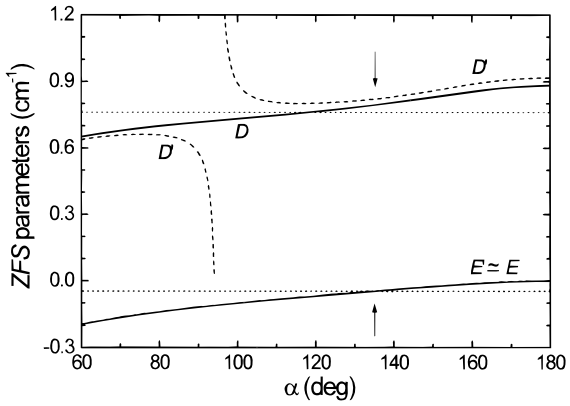

Figure 12. Triplet carbene. "Spin−spin-only" (*D*, *E*, CISD/D95**, solid lines) and "spin−spin plus spin−orbit" (*D*′, *E*′, spin−orbit coupling with six lowest singlets with CASSCF(6,6)/D95**, dashed lines) zero-field splitting parameters at triplet-optimized geometries as a function of the valence angle α. Best experimental *D*′ and *E*′ values are shown by dotted lines. The optimized value of α is marked by arrows. The EPR axis labeling convention[19] is used.

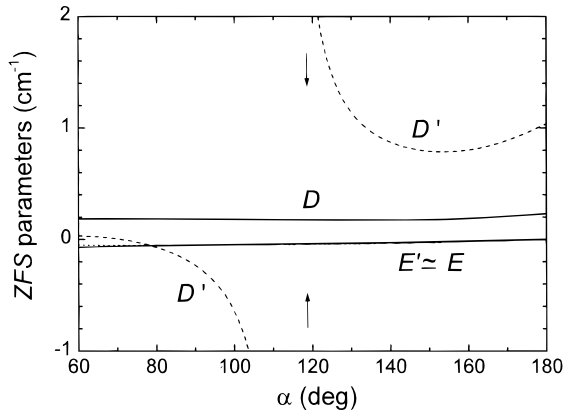

Figure 13. Triplet silylene. "Spin−spin-only" (*D*, *E*, CISD/D95**, solid lines) and "spin−spin plus spin−orbit" (*D*′, *E*′, spin−orbit coupling with six lowest singlets with CASSCF(6,6)/D95**, dashed lines) zero-field splitting parameters at triplet-optimized geometries as a function of the valence angle α. The optimized value of α is marked by arrows. The EPR axis labeling convention[19] is used.

of the spin−orbit matrix elements $\langle T_u|H^{SO}|S_i\rangle$, where $u = x, y$, or z, and $i = 0-5$. The resulting *D*′ and *E*′ values (Figures 12 and 13, the EPR convention for axis labels) were computed in the usual manner (Figure 1) from the eigenvalues *X*′, *Y*′, and *Z*′ obtained by diagonalization of the Hamiltonian matrix containing both types of elements, even at geometries at which the singlet and triplet energies are very close. Therefore, they exhibit a discontinuity at the crossing points, where *D*′ and *E*′ are not defined. As noted in the section on Calculational Procedures, this is artificial in that it assumes a three-level system even at the crossing point, and the singularity would disappear upon proper treatment of what actually is a four-level system in terms of *D*, *E*, *J*, and spin−orbit coupling matrix elements.

Atomic and Natural Hybrid Orbital Pair Contributions. Atomic contributions from the hydrogen atoms to all spin−orbit coupling matrix elements are negligible. Figure 14 shows the decomposition of the only nonvanishing component of the spin−orbit matrix element between the lowest triplet and the lowest singlet state in CH_2, $\langle T_y|H^{SO}|S_i\rangle$ in the usual axis labeling convention, into contributions from various natural hybrid pairs. In these, one member of a pair contributes to one of the nonbonding orbitals (A) and the other member contributes to

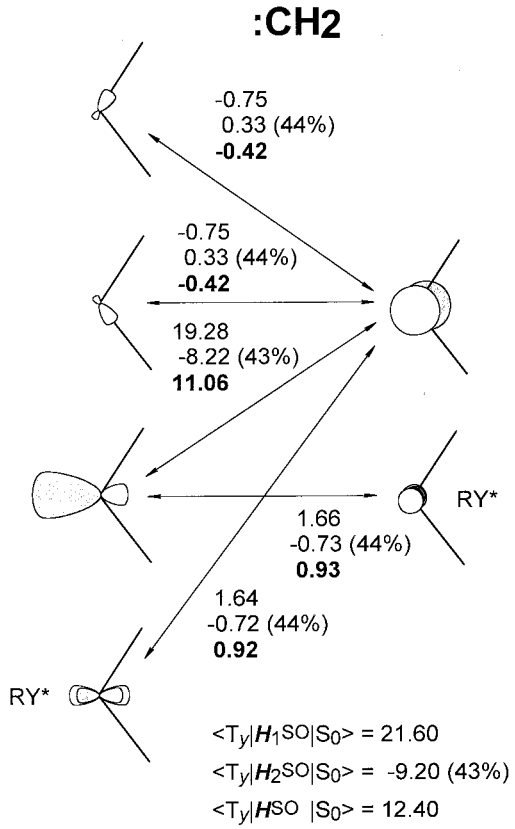

Figure 14. Triplet carbene at optimized geometry. Contributions from natural hybrid orbital pairs to the spin−orbit matrix element $\langle T_y|\hat{H}^{SO}|S_0\rangle$, with the usual axis labeling convention. For each pair of hybrid orbitals connected by an arrow, the one-electron part, the two-electron part, and, in bold, the total contribution of the pair to the value of the matrix element, respectively, are listed from top to bottom. Sums of contributions from all orbital pairs are listed underneath, in the same order. CASSCF(6,6)/D95**.

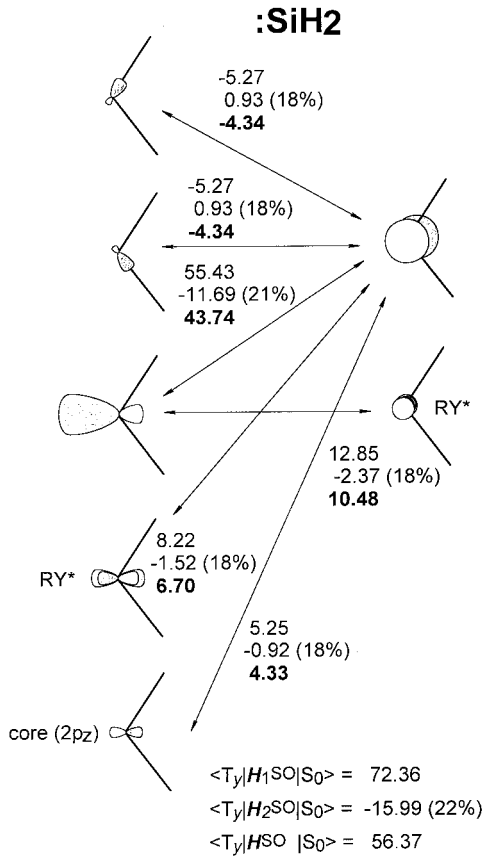

Figure 15. Triplet silylene at optimized geometry. See caption to Figure 14.

the other nonbonding orbital (B) of the biradical. Figure 15 shows analogous results for SiH_2.

One- and Two-Electron Contributions to Spin−Orbit Coupling Matrix Elements. As expected, the two-electron contributions to the spin−orbit matrix elements are opposed in sign to the one-electron contributions. In CH_2, they are roughly half their size (51%) and, in SiH_2, roughly one-fourth their size (23%) for all geometries. These percentages apply not only to the total size of these matrix elements but also separately to all the important contributions from each hybrid orbital pair (Figures 14 and 15). Only the small and insignificant contributions show more variability. Such constancy in the total size and in the important contributions supports the common usage of an effective one-electron operator for spin−orbit coupling, but it is not obvious that this result is general.

Discussion

Electronic States. The trends in potential energy curves of the lowest four states shown in Figure 6 (carbene) and Figure 7 (silylene), obtained at geometries optimized for the lowest triplet, agree with expectations based on measurements (carbene,[12,48−52] silylene[48,51,53−55]) and with more accurate calculations (carbene,[11,56−68] silylene[11,45,57,68−72]) performed separately at the optimized geometries of each individual state. The higher states are not rendered correctly since diffuse orbitals are absent in the basis set used (triplet carbene is ionized at 10.396 eV[73] and eight Rydberg states converging to it have been identified;[74,75] singlet silylene is ionized at 9.15 eV[55]). This is immaterial for our purposes since we are merely interested in states that affect the lowest triplet significantly through spin−orbit coupling. (Figure 4 shows that the inclusion of diffuse functions in the basis has only a small effect on the spin−orbit matrix elements, even for the higher singlets.) The reason for including the inaccurately calculated high-energy states in Figures 6 and 7 at all is that at certain values of the valence angle α they drop in energy and become valence in nature.

The general features of the potential energy curves for the states of CH_2 and SiH_2 are very similar. (We use the usual choice of axis labels.) The primary difference is in the relative location of the lowest triplet ($^3B_1$) and the lowest singlet (1^1A_1) curves. In CH_2 they cross at 95° and the absolute minimum is in the $^3B_1$ surface, whereas in SiH_2, they cross at 128° and the absolute minimum is in the 1^1A_1 surface. (It does not appear in Figure 7 since there the bond lengths are optimized for the triplet.) The crossing is weakly avoided due to spin−orbit coupling, at least for some of the triplet sublevels. Thus, it appears that carbene actually may formally have two ground-state isomers (i.e., two local minima in the lowest potential energy surface separated by a very small potential energy barrier and differing in multiplicity, as opposed to a single local minimum in the lowest potential energy surface and another minimum in a low-lying electronically excited state of different multiplicity; the distinction would disappear if one abandoned the Born−Oppenheimer approximation). The more stable isomer is moderately bent and has a triplet $^3B_1$ ground state. The other lies 9.215 kcal/mol higher,[49] is strongly bent, and has a singlet $^1A_1$ ground state. (Its absolute minimum does not appear in Figure 6 since there the bond lengths are optimized for the triplet.) Silylene probably has only one isomer, strongly bent, with a $^1A_1$ singlet ground state, since the region of most favorable triplet geometries most likely corresponds only to a

shoulder and not a minimum in the lowest potential energy surface. (The 1^1A_1 curve cuts the $^3B_1$ curve close to the minimum in the latter, and spin−orbit coupling is stronger.) A more thorough examination by a higher level method in all three dimensions of the nuclear configuration space of SiH_2 would be required to settle the number of formal Born−Oppenheimer isomers definitively. There is little doubt, however, that the lifetime of isolated vibrationally cold triplet silylene will be shorter than that of isolated vibrationally cold singlet carbene, and the former has not been observed so far.

If two sufficiently bulky but otherwise inert substituents R could be introduced to form SiR_2, the energies of all states would be raised roughly equally on the left-hand side of Figure 7, and a minimum would appear in the ground-state energy surface near a bend angle of 130°, where triplet is the ground state.[69] In such a case, a species with zero-field splitting parameters approximately equal to those presently calculated would presumably be observable by Q-band EPR.

Spin−Orbit Coupling and Intersystem Crossing. This, too, is best discussed in the usual notation for molecular axes, in which *z* is the 2-fold symmetry axis and *x* is the out-of plane axis. The lowest triplet T_1 states of CH_2 and SiH_2 have B_1 spatial symmetry in the C_{2v} group, and the total wave functions of their three components transform as A_2 (T_x), A_1 (T_y), and B_2 (T_z). In both molecules, at the geometry corresponding to the triplet minimum, the symmetry of the S_0, S_2, and S_5 singlet states is A_1, and these states spin−orbit couple with the T_y sublevel of T_1. In both molecules, the S_3 state has symmetry A_2 and the S_4 state has symmetry B_2, and they spin−orbit couple with the T_x and T_z sublevels of T_1, respectively. In both cases, the S_1 singlet state is of symmetry B_1 and does not spin−orbit couple with T_1 at all in the absence of vibrational perturbations.

Intersystem crossing from T_1 to S_0 therefore selectively depopulates the T_y sublevel of T_1, and intersystem crossing from S_0 to T_1 selectively populates it. The magnitude of the spin−orbit coupling element changes only a little as a function of the valence angle from 60° to 130° or 140°, and is 4−5 times larger for silylene than for carbene. Using the Fermi golden rule, this would provide an inherent acceleration of intersystem crossing in silylene by a factor of about 20 if the Franck−Condon weighted densities of states were the same. Even in carbene, the magnitude of the spin−orbit coupling element, about 12 cm^{-1}, is over an order of magnitude larger than in biradicals that do not carry both radical centers on the same carbon atom, and both molecules are extraordinarily well set up for intersystem crossing.

Spin−Orbit Coupling and Zero-Field Splitting. Of all singlet states, S_0 is by far the closest in energy to the T_1 state, and the spin−orbit mixing of these two states is the most important both in CH_2 and in SiH_2. The triplet sublevel that is expected to be shifted the most by spin−orbit coupling, T_y in the usual notation, corresponds to the axis that is parallel to the H−H line, labeled *z* in the EPR convention. We therefore need to label it T_z when referring to Figure 1. The other two sublevels are not expected to be shifted much by interaction with the singlets S_3 and S_4, whose spin−orbit coupling elements with T_1 are somewhat smaller and which are much farther in energy. Spin−orbit coupling should therefore have nearly no effect on their separation, and E and E' should be nearly identical.

Since $D > 0$, $E < 0$ holds for carbene and silylene, the top part of Figure 1 applies, and in the EPR convention for axis labels, T_z is the lowest of the three sublevels. When T_1 lies below S_0 in energy, as is the case in carbene at its equilibrium geometry, T_1-S_0 spin−orbit coupling should stabilize T_z relative to the average of T_x and T_y and thus make D' larger than D. When S_0 lies below T_1 in energy, as is the case in silylene at its equilibrium geometry, T_1-S_0 spin−orbit coupling should destabilize T_z relative to the average of T_x and T_y and thus make D' smaller than D. These qualitative expectations are borne out by the numerical results shown in Figures 12 and 13. At geometries close to linear, the above argument does not hold, since the T_1-S_0 spin−orbit coupling element is small and vanishes altogether at the linear geometry. At these valence angles the T_1-S_2 spin−orbit coupling element is particularly large and the T_1-S_2 energy gap is reduced. As a result, S_2 takes over the role played by S_0 at smaller valence angles, and the increase from D to D' still occurs. (In silylene, the difference actually increases as the linear geometry is approached.)

It is seen in Figures 12 and 13 that at most geometries the effects of spin−orbit coupling on the zero-field splitting parameters are minor in carbene and dominant in silylene. The reasons for the difference are readily understood. In triplet carbene, the "spin−spin-only" zero-field splitting of the three triplet sublevels, described by the D and E values, is already unusually large since both unpaired electrons reside in relatively small orbitals located at the same atom, and even a quite significant shift in the energy of the T_z sublevel due to spin−orbit coupling appears to be relatively minor. In silylene, the D and E values are 3−4 times smaller since the silicon orbitals holding the unpaired electrons are larger, and spin−orbit coupling matrix element is now 4−5 times larger (heavy atom effect). These differences are sufficient to make carbene "spin−spin dominated" and silylene "spin−orbit dominated" at most geometries. We shall therefore discuss the two molecules separately.

Carbene. Our CISDTQ/cc-pVDZ "spin−spin-only" values for carbene at its optimized triplet geometry are $D = 0.8043$ cm^{-1} and $E = -0.0428$ cm^{-1}, and results obtained at the CISD level are nearly identical (Figure 2). In agreement with the prior work,[18] corrections for the effect of spin−orbit coupling are small: $D' = D + 0.023$ cm^{-1}, $E' = E + 0.0001$ cm^{-1}. With the exception of STO-3G, which does very poorly, even moderately sized basis sets thus seem to be quite satisfactory for the evaluation of zero-field splitting, provided that extensive electron correlation is introduced in the spin−spin dipolar interaction part of the calculation. The agreement for E' is essentially exact, and the value of D' is only 10% too high. It is somewhat disturbing, though, that there is no indication that improvement in either the basis set (Figure 2) or the description of electron correlation (Figure 3) will bring about convergence to the experimental value of D'. It would be somewhat surprising if the neglect of vibrational averaging alone were responsible for the remaining discrepancy.

The trends in the zero-field splitting parameters computed as a function of the valence angle α agree with those suggested by the earlier work.[17,18] Upon going from 180° to 60°, the "spin−spin-only" value D is reduced by nearly one-third (Figure 8). The full value, D', runs parallel to D and is only slightly larger until α approaches the seam of first-order triplet−singlet crossing. Starting at 110° or so, D' begins to increase rapidly and ultimately diverges when the crossing seam is reached at 95°. At even smaller angles, D' rises from very negative values and joins D quite closely once again as α reaches a value of about 80°.

As noted above, very close to the crossing point (actually, a two-dimensional crossing seam) the EPR spectrum would involve transitions between four rather than three levels, and it would not have the usual appearance, making the experimental

value of D' undefined. However, even carbenes with valence angles somewhat further from the crossing region and with quite ordinary EPR spectra should exhibit unusual D' values. Sterically constrained but otherwise electronically unperturbed triplet carbenes with such small valence angles have not been observed so far, but might be accessible in the future. A reliable prediction of their zero-field splitting parameters would require a calculation over a range of values of all three geometrical parameters that define structure at the carbene carbon and averaging over vibrational wave functions.

The E and E' values calculated for triplet CH_2 are essentially identical to each other at all values of the valence angle. They vanish at 180° by symmetry and grow steadily more negative as α decreases, to a value as large as -0.2 cm^{-1} at 60°.

Silylene. The results predicted for triplet SiH_2 are quite different. The "spin−spin-only" values D and E are smaller in absolute value (Figure 9). Upon reducing the valence angle α from 180° to 140°, D is reduced from 0.23 to 0.17 cm^{-1} and then rises slowly to 0.18 as α is reduced to 60°. The E value vanishes at $\alpha = 180°$ by symmetry and grows negative as the molecule is bent, to a value of -0.07 cm^{-1} at $\alpha = 60°$.

As in carbene, the spin−orbit correction to E is totally negligible. In contrast to carbene, however, spin−orbit effects dominate the D' value (Figure 13). The matrix element $\langle T_y|\hat{H}^{SO}|S_0\rangle$ is so large that the effect of the first-order triplet−singlet crossing at $\alpha = 128°$ permeates the whole range of α values. At larger α values, where the T_1 state lies below S_0, T_z is preferentially stabilized and D' is much larger than D, while at smaller α values, where T_1 lies below S_0, T_z is preferentially destabilized and D' is much smaller than D. As noted above, the even much larger value of the $\langle T_y|\hat{H}^{SO}|S_2\rangle$ element at nearly linear geometries (Figure 11) causes an additional stabilization of T_y and a further increase in D', even though the T_1-S_2 separation remains relatively large.

For a reliable prediction of zero-field splitting parameters of silylenes containing bulky but noninteracting substituents that have a large valence angle at equilibrium and a triplet ground state,[69] vibrational averaging would again be necessary. Clearly, however, in an otherwise unperturbed silylene with a valence angle in the vicinity of 120°, D' values on the order of 1−3 cm^{-1} can be expected, and observation of an EPR signal on an X-band spectrometer may well be impossible. In contrast, excited triplet silylenes forced to adopt a valence angle of less than 90° by a suitable structural constraint should have quite small D' values.

Analysis of Results in Terms of a Simple Model. In Part 1[1] three conditions for the S_0-T_1 spin−orbit coupling vector ($\langle T_x|\hat{H}^{SO}|S_0\rangle$, $\langle T_y|\hat{H}^{SO}|S_0\rangle$, $\langle T_z|\hat{H}^{SO}|S_0\rangle$) in an organic biradical to be large were deduced from a simple algebraically soluble model based on the ^{1,3}(AB), $^1(A^2 + B^2)$, and $^1(A^2 - B^2)$ configurations built from the most localized orbitals A and B singly occupied in the triplet state. They are as follows: (i) The orbitals A and B should interact covalently through a nonzero resonance integral and/or be sufficiently different in energy for one of them to have electron occupancy near two in S_0 (the spin−orbit coupling vector is proportional to the coefficient of the $A^2 + B^2$ configuration in S_0). (ii) The biradical should contain one or more high-Z atoms at which one p orbital contributes strongly to A and another to B. (Each such atom provides a vectorial contribution proportional to its atomic spin−orbit coupling constant and directed along an axis perpendicular to those of the two p orbitals; its size and sense are dictated by the coefficients with which the two p orbitals enter A and B.) (iii) If several such atoms are present, these coefficients should be such that the atomic contributions add rather than cancel. In this simplest formulation, two-center contributions were neglected, but their qualitative effect can be added easily if needed.

The application of these results to carbene and silylene is straightforward. The orbitals A and B are the b_1 symmetry p orbital on C or Si that is directed along x and the a_1 symmetry hybrid orbital directed along the 2-fold symmetry axis z. The resonance integral between them vanishes by symmetry, and condition (i) can be fulfilled only when the valence angle is less than 180°, since the two orbitals then differ in energy. Indeed, the calculated S_0-T_1 spin−orbit coupling vector is large at small valence angles, where the a_1 orbital has significant s character, and drops to zero as the valence angle approaches 180° and both orbitals become purely p and equivalent (Figures 10 and 11). As expected, the calculated S_0 and S_2 singlet states of carbene and silylene are predominantly mixtures of $A^2 + B^2$ and $A^2 - B^2$ configurations, while in the S_1 state the AB configuration dominates. The coefficients of $A^2 + B^2$ and $A^2 - B^2$ depend on the valence angle in the way anticipated from the simple model. In S_0 the coefficient of $A^2 + B^2$ (0.43 at the triplet minimum of CH_2) decreases with the increasing bond angle and vanishes at the linear geometry, whereas the S_2 state has maximum coefficient (0.99) at the linear geometry, and it decreases with decreasing bond angle (0.87 at triplet minimum). The other three singlet states have zero or negligible contributions from the $A^2 + B^2$, $A^2 - B^2$, and AB configurations.

Condition (ii) is clearly fulfilled, since one of the orbitals A and B is a p orbital on the C or an Si atom, and the other contains a large contribution from another p orbital on the same atom, particularly for large valence angles. The direction of the vectorial contribution from this atom is directed along the y axis, in agreement with a simple symmetry analysis and with calculations. The larger Z number of Si is responsible for the larger spin−orbit coupling vector in silylene (heavy atom effect). Condition (iii) does not need to be considered, since the molecules contain only one high-Z atom.

The present results permit a more quantitative analysis of the way in which condition (ii) is fulfilled, by decomposition of the vectorial contribution from the C or Si atom into contributions from pairs of orbitals used as a basis set for the description of the orbitals A and B. Although an atomic orbital basis set could be used for this purpose, this is unwieldy and uninformative when large basis sets are used. Analysis in terms of Weinhold's[7] natural atomic, hybrid, or bond orbitals, both preorthogonal (PNHO, PNBO, PNAO) and orthogonal (NHO, NBO, NAO), minimizes the number of contributions and is intuitively appealing. The optimal selection depends on the actual system, its symmetry, and bonding pattern. We find that in orthogonal bases the number of important pair contributions is usually smaller, but the members of these basis sets are somewhat delocalized and more difficult to understand in simple chemical terms. We find it most instructive to use preorthogonal natural hybrid orbitals (Figures 14 and 15).

For both molecules the important contributions to the S_0-T_1 spin−orbit coupling vector (98% or more) originate from pairs of hybrid orbitals localized on the central atom. The largest contribution by far is due to the pair of hybrids representing the radical centers in the simplest description of the molecules, one pure p orbital and the other an s−p hybrid. As expected from the simple model, the contribution increases with the increasing p character of the hybrid as the valence angle is opened wider, since this leads to better overlap with the other hybrid orbital rotated by 90° about y. However, simultaneously, the $A^2 + B^2$ character of the S_0 wave function decreases and

condition (i) is fulfilled less well. For a large range of valence angles, these effects cancel, and the spin−orbit coupling vector is nearly independent of the valence angle (Figures 10 and 11). Close to the linear geometry, the contribution from $A^2 + B^2$ to S_0 drops abruptly, and the S_0-T_1 spin−orbit coupling vector vanishes.

Summary of Computational Requirements. The results for carbene show that the results of spin−spin dipolar coupling calculations converge slowly with increasing basis set quality. At least a DZ basis set is needed for semiquantitative results (Figure 2). The results are sensitive to the description of electron correlation. The CIS and CASSCF(6,6) methods are of questionable value. CISD provides good results, which change little if triple and quadruple excitations are added (Figure 3). Not surprisingly, for highly accurate results it is necessary to combine at least a CISD level of electron correlation with a very large basis set.

The results of spin−orbit coupling calculations show little dependence on basis set quality provided that at least DZ quality is used (Figure 4). Only limited conclusions can be drawn concerning the effect of electron correlation, because our computer could handle at most CASSCF(6,6) when this work was performed. From the sequence of CAS calculations in Figure 5 it seems that a better level of correlation is needed if the results are to be really accurate, but qualitative features are well described already with smaller active spaces.

Acknowledgment. This work was supported by the NSF (Grants CHE-9318469 and CHE-9412767). We are grateful to Professors H. F. King, J. W. McIver, Jr., R. A. Caldwell, and E. R. Davidson for providing us with sections of computer code that served as the basis for writing the computer program used in the present study.

References and Notes

(1) Part 1: Michl, J. *J. Am. Chem. Soc.* **1996**, *118*, 3568.

(2) Salem, L.; Rowland, C. *Angew. Chem., Int. Ed. Engl.* **1972**, *11*, 92.

(3) For a review, see: Klessinger, M. In *Theoretical Organic Chemistry*; Parkanyi, C., Ed.; Theoretical and Computational Chemistry, Vol. 5; Elsevier: Amsterdam, The Netherlands, 1988; p 581.

(4) Michl, J.; Downing, J. W. Presented at the 5th IAPS Winter Conference, Clearwater Beach, FL, 2−6 January, 1993, Abstract C3.

(5) Yarkony, D. R. *Int. Rev. Phys. Chem.* **1992**, *11*, 195.

(6) Zimmerman, H. E.; Kutateladze, A. G. *J. Am. Chem. Soc.* **1996**, *118*, 249.

(7) Reed, A. E.; Weinstock, R. B.; Weinhold, F. *J. Chem. Phys.* **1985**, *83*, 735. Reed, A. E.; Curtiss, L. A.; Weinhold, F. *Chem. Rev.* **1988**, *88*, 899.

(8) The analysis of contributions to the SOC in terms of the NHOs was developed independently by Zimmerman and Kutateladze.[6] The neglect of three- and four-center terms introduced by these authors in the analysis of the two-electron contributions is avoided in our procedure.

(9) Carlacci, L.; Doubleday, C., Jr.; Furlani, T. R.; King, H. F.; McIver, J. W., Jr. *J. Am. Chem. Soc.* **1987**, *109*, 5323.

(10) McKinley, A. J.; Ibrahim, P. N.; Balaji, V.; Michl, J. *J. Am. Chem. Soc.* **1992**, *114*, 10631.

(11) Matsunaga, N.; Koseki, S.; Gordon, M. S. *J. Chem. Phys.* **1996**, *104*, 7988.

(12) McKellar, A. R. W.; Bunker, P. R.; Sears, T. J.; Evenson, K. M.; Saykally, R. J.; Langhoff, S. R. *J. Chem. Phys.* **1983**, *79*, 5251.

(13) Duxbury, G.; Jungen, C. *Mol. Phys.* **1988**, *63*, 981. Alijah, A.; Duxbury, G. *Mol. Phys.* **1990**, *70*, 605.

(14) Duxbury, G.; Alijah, A.; Trieling, R. R. *J. Chem. Phys.* **1993**, *98*, 811.

(15) Higuchi, J. *J. Chem. Phys.* **1963**, *38*, 1237; **1963**, *39*, 1339.

(16) Harrison, J. F. *J. Chem. Phys.* **1971**, *54*, 5413.

(17) Langhoff, S. R.; Davidson, E. R. *Int. J. Quantum Chem.* **1973**, *7*, 759.

(18) Langhoff, S. R. *J. Chem. Phys.* **1974**, *61*, 3881.

(19) Weltner, W., Jr. *Magnetic Atoms and Molecules*; Van Nostrand Rheinhold: New York, 1983; Chapter 3.

(20) Nolte, J.; Temps, F.; Wagner, H. Gg.; Wolf, M.; Sears, T. J. *J. Chem. Phys.* **1994**, *100*, 8706.

(21) Dupuis, M.; Spangler, D.; Wendoloski, J. J. *Program QG01*; National Resource for Computations in Chemistry, Software Catalog, University of California: Berkeley, CA, 1980. Schmidt, M. W.; Baldridge, K. K.; Boatz, J. A.; Elbert, S. T.; Gordon, M. S.; Jensen, J. H.; Koseki, S.; Matsunaga, N.; Nguyen, K. A.; Su, S. J.; Windus, T. L.; Dupuis, M.; Montgomery, J. A. *J. Comput. Chem.* **1993**, *14*, 1347.

(22) Davidson, E. R.; Feller, D. MELD, Indiana University, Bloomington, IN (version distributed in METECC 94).

(23) Gaussian 94, Revision E.2: Frisch, M. J.; Trucks, G. W.; Schlegel, H. B.; Gill, P. M. W.; Johnson, B. G.; Robb, M. A.; Cheeseman, J. R.; Keith, T.; Petersson, G. A.; Montgomery, J. A.; Raghavachari, K.; Al-Laham, M. A.; Zakrzewski, V. G.; Ortiz, J. V.; Foresman, J. B.; Cioslowski, J.; Stefanov, B. B.; Nanayakkara, A.; Challacombe, M.; Peng, C. Y.; Ayala, P. Y.; Chen, W.; Wong, M. W.; Andres, J. L.; Replogle, E. S.; Gomperts, R.; Martin, R. L.; Fox, D. J.; Binkley, J. S.; Defrees, D. J.; Baker, J.; Stewart, J. P.; Head-Gordon, M.; Gonzalez, C. J. A. Pople, Gaussian, Inc., Pittsburgh, PA, 1995.

(24) CADPAC: The Cambridge Analytic Derivatives Package Issue 6, Cambridge, 1995. A suite of quantum chemistry programs developed by R. D. Amos with contributions from I. L. Alberts, J. S. Andrews, S. M. Colwell, N. C. Handy, D. Jayatilaka, P. J. Knowles, R. Kobayashi, K. E. Laidig, G. Laming, A. M. Lee, P. E. Maslen, C. W. Murray, J. E. Rice, E. D. Simandiras, A. J. Stone, M.-D. Su, and D. J. Tozer.

(25) Ellis, R. L.; Jaffé, H. H. In *Modern Theoretical Chemistry*; Segal, G., Ed.; Plenum: New York, 1977; Vol. 8, p 74.

(26) Böckmann, M.; Klessinger, M.; Zerner, M. C. *J. Phys. Chem.* **1996**, *100*, 10570.

(27) Prasad, B. L. V.; Radhakrishnan T. P. *J. Phys. Chem.* **1992**, *96*, 9232.

(28) Furlani, T. Ab Initio Calculation of Spin−Orbit Coupling Constants in Polyatomic Molecules. Ph.D. Dissertation, State University of New York at Buffalo, 1985.

(29) Bearpark, M. J.; Handy, N. C.; Palmieri, P.; Tarroni, R. *Mol. Phys.* **1993**, *80*, 479.

(30) Vahtras, O.; Ågren, H.; Jørgensen, P.; Jensen, H. J. A.; Helgaker, T.; Olsen, J. *J. Chem. Phys.* **1992**, *96*, 2118; **1992**, *97*, 9178.

(31) Knuts, S.; Minaev, B. F.; Vahtras, O.; Ågren, H. *Int. J. Quantum Chem.* **1995**, *55*, 23.

(32) Marian, C. M.; Ippe, D.; Hess, B. A.; Peyerimhoff, S. D. *Theor. Chim. Acta* **1992**, *81*, 375.

(33) Glendening, E. D.; Badenhoop, J. K.; Reed, A. E.; Carpenter, J. E.; Weinhold, F. NBO 4.0, Theoretical Chemistry Institute, University of Wisconsin, Madison, WI, 1994.

(34) Caldwell, R. A.; Jacobs, L. D.; Furlani, T. R.; Nalley, T. A.; Laboy, J. *J. Am. Chem. Soc.* **1992**, *114*, 1623.

(35) Michl, J.; Havlas, Z. *Pure Appl. Chem.* **1997**, *69*, 785.

(36) Havlas, Z.; Michl, J. *J. Mol. Struct. (THEOCHEM)* **1997**, *398*−*399*, 281.

(37) Zimmerman, H. E.; Kutateladze, A. G.; Maekawa, Y.; Mangette, J. E. *J. Am. Chem. Soc.* **1994**, *116*, 9795.

(38) Bonačić-Koutecký, V.; Koutecký, J.; Michl, J. *Angew. Chem., Int. Ed. Engl.* **1987**, *26*, 170.

(39) Langhoff, S. R.; Kern, C. W. In *Applications of Electronic Structure Theory*; Schaefer, H. F., Ed.; Plenum: New York, 1977; p 381. Bethe, H. A.; Salpeter, E. E. *Quantum Mechanics of One- and Two-Electron Atoms*; Springer-Verlag: Berlin, 1957. Hirschfelder, J. O.; Curtiss, C. F.; Bird, R. B. *Molecular Theory of Gases and Liquids*; John Wiley: New York, 1954.

(40) Davidson, E. R.; Ellenbogen, J. C.; Langhoff, S. R. *J. Chem. Phys.* **1980**, *73*, 865.

(41) King, H. F.; Furlani, T. R. *J. Comput. Chem.* **1988**, *9*, 771.

(42) Shavitt, I. In *Methods of Electronic Structure Theory*; Schaefer, H. F. III, Ed.; Plenum: New York, Vol. 3, p 205.

(43) Patel-Misra, D.; Parlant, G.; Sauder, D. G.; Yarkony, D. R.; Dagdigian, P. J. *J. Chem. Phys.* **1991**, *94*, 1913.

(44) Bunker, P. R.; Jensen, P.; Kraemer, W. P.; Beardsworth, R. *J. Chem. Phys.* **1986**, *85*, 3724.

(45) Gabriel, W.; Rosmus, P.; Yamashita, K.; Morokuma, K.; Palmieri, P. *Chem. Phys.* **1993**, *174*, 45.

(46) King, H. F.; Stanton, R. E.; Kim, H.; Wyatt R. E.; Parr, R. G. *J. Chem. Phys.* **1967**, *47*, 1936.

(47) Lengsfield, B. H., III.; Jafri, J. A.; Phillips, D. H.; Bauschlicher, C. W., Jr. *J. Chem. Phys.* **1981**, *74*, 6849.

(48) Herzberg, G. *Electronic Spectra and Electronic Structure of Polyatomic Molecules*, Van Nostrand: Princeton, NJ, 1967; pp 491, 493.

(49) Jensen, P.; Bunker, P. R. *J. Chem. Phys.* **1988**, *89*, 1327.

(50) Hartland, G. V.; Qin, D.; Dai, H.-L. *J. Chem. Phys.* **1993**, *98*, 2469.

(51) Cramer, C. J.; Dulles, F. J.; Storer, J. W.; Worthington, S. E. *Chem. Phys. Lett.* **1994**, *218*, 387.

(52) Leopold, D. G.; Murray, K. K.; Stevens Miller, A. E.; Lineberger, W. C. *J. Chem. Phys.* **1985**, *83*, 4849.

(53) Milligan, D. E.; Jacox, M. E. *J. Chem. Phys.* **1970**, *52*, 2594.

(54) Kashdan, A.; Herbst, E.; Lineberger, W. C. *J. Chem. Phys.* **1975**, *62*, 541.
(55) Berkowitz, J.; Greene, J. P.; Cho, H.; Ruscic, B. *J. Chem. Phys.* **1987**, *86*, 1235.
(56) Green, W. H., Jr.; Handy, N. C.; Knowles, P. J.; Carter, S. *J. Chem. Phys.* **1991**, *94*, 118.
(57) Apeloig, Y. In *The Chemistry of Organic Silicon Compounds*; Patai, S., Rappoport, Z., Eds.; John Wiley & Sons Ltd.: Chichester, 1989; Part 1, p 167 ff.
(58) Andrews, J. S.; Murray, C. W.; Handy, N. C. *Chem. Phys. Lett.* **1993**, *201*, 458.
(59) Koch, H.; Christiansen, O.; Jørgensen, P.; Olsen, J. *Chem. Phys. Lett.* **1995**, *244*, 75.
(60) Li, X.; Piecuch, P.; Paldus, J. *Chem. Phys. Lett.* **1994**, *224*, 267.
(61) Piecuch, P.; Li, X.; Paldus, J. *Chem. Phys. Lett.* **1994**, *230*, 377.
(62) Miralles, J.; Castell, O.; Caballol, R.; Malrieux, J. P. *Chem. Phys.* **1993**, *172*, 33.
(63) Bunker, P. R.; Jensen, P.; Yamaguchi, Y.; Schaefer, H. F., III *J. Phys. Chem.* **1996**, *100*, 18088.
(64) Balková, A.; Bartlett, R. J. *J. Chem. Phys.* **1995**, *102*, 7116.
(65) Yamaguchi, Y.; Sherrill, C. D.; Schaefer, H. F., III *J. Phys. Chem.* **1996**, *100*, 7911.
(66) Yamaguchi, Y.; Schaefer, H. F., III *J. Chem. Phys.* **1997**, *106*, 1819.
(67) Sherrill, C. D.; Van Huis, T. J.; Yamaguchi, Y.; Schaefer, H. F., III *J. Mol. Struct. (THEOCHEM)* **1997**, *400*, 139.
(68) Bauschlicher, C. W.; Langhoff, S. R.; Taylor, P. R. *J. Chem. Phys.* **1987**, *87*, 387.
(69) Grev, R. S.; Schaefer, H. F., III.; Gaspar, P. P. *J. Am. Chem. Soc.* **1991**, *113*, 5638.
(70) Selmani, A.; Salahub, D. R. *J. Chem. Phys.* **1988**, *89*, 1529.
(71) Koseki, S.; Gordon, M. S. *J. Mol. Spectrosc.* **1987**, *123*, 392.
(72) Rice, J. E.; Handy, N. C. *Chem. Phys. Lett.* **1984**, *107*, 365.
(73) Herzberg, G. *Can. J. Phys.* **1961**, *39*, 1511.
(74) Irikura, K. K.; Hudgens, J. W. *J. Phys. Chem.* **1992**, *96*, 518.
(75) Irikura, K. K.; Johnson, R. D., III.; Hudgens, J. W. *J. Phys. Chem.* **1992**, *96*, 6131.